Ann Surg Oncol (2019) 26:1833–1840
https://doi.org/10.1245/s10434-018-07133-6

Annals of
SURGICAL ONCOLOGY
OFFICIAL JOURNAL OF THE SOCIETY OF SURGICAL ONCOLOGY

ORIGINAL ARTICLE – HEPATOBILIARY TUMORS

Fluorescent Tissue Assessment of Colorectal Cancer Liver Metastases Ablation Zone: A Potential Real-Time Biomarker of Complete Tumor Ablation

Vlasios S. Sotirchos, MD[1], Sho Fujisawa, PhD[2], Efsevia Vakiani, MD, PhD[3], Stephen B. Solomon, MD, FSIR[4], Katia O. Manova-Todorova, PhD[2], and Constantinos T. Sofocleous, MD, PhD, FSIR, FCIRSE[4]

[1]Department of Radiology, Hospital of the University of Pennsylvania, Philadelphia; [2]Molecular Cytology, Memorial Sloan Kettering Cancer Center, New York, NY; [3]Department of Pathology, Memorial Sloan Kettering Cancer Center, New York, NY; [4]Interventional Radiology Service, Memorial Sloan Kettering Cancer Center, New York, NY

ABSTRACT

Background. This study aimed to evaluate whether rapid fluorescent tissue examination immediately after colorectal cancer liver metastasis (CLM) ablation correlates with standard pathologic and immunohistochemical (IHC) assessments.

Methods. This prospective, National Institutes of Health-supported study enrolled 34 consecutive patients with 53 CLMs ablated between January 2011 and December 2014. Immediately after ablation, core needle sampling of the ablation zone was performed. Tissue samples were evaluated with fluorescent viability (MitoTracker Red) and nuclear (Hoechst) stains. Confocal microscope imaging was performed within 30 min after ablation. The same samples were subsequently fixed and stained with hematoxylin and eosin (H&E). Identified tumor cells underwent IHC staining for proliferation (Ki67) and viability (OxPhos). The study pathologist, blinded to the H&E and IHC assessment, evaluated the fluorescent images separately to detect viable tumor cells. Sensitivity, specificity, and overall concordance of the fluorescent versus H&E and IHC assessments were calculated.

Results. A total of 63 tissue samples were collected and processed. The overall concordance rate between the immediate fluorescent and the subsequent H&E and IHC assessments was 94% (59/63). The fluorescent assessment sensitivity and specificity for the identification of tumor cells were respectively 100% (18/18) and 91% (41/45).

Conclusions. The study showed a high concordance rate between the immediate fluorescent assessment and the standard H&E and IHC assessment of the ablation zone. Given the documented prognostic value of ablation zone tissue characteristics for outcomes after ablation of CLM, the fluorescent assessment offers a potential intra-procedural biomarker of complete tumor ablation.

Colorectal cancer is the most common gastrointestinal malignancy and the second most common cause of cancer-related death.[1] A significant percentage of patients experience colorectal liver metastases (CLMs) during the course of their disease.[2]

Although hepatic resection is considered the treatment of choice for CLM, only up to 20% of patients are surgical candidates due to the extent of hepatic disease, the presence of significant extrahepatic tumor burden, and comorbid conditions.[3,4] Percutaneous image-guided tumor ablation is an alternative treatment with documented safety and efficacy for selected patients with relatively small hepatic tumors.[5,6] The limitations of percutaneous ablative techniques include incomplete tumor treatment and local tumor progression (LTP).[5–8] Therefore, it is crucial to develop prognostic markers that can be applied in real time to identify patients at increased risk for incomplete treatment and LTP after ablation. Such markers can guide decisions regarding additional ablations within the same treatment session or indicate the need for early administration of adjuvant therapies.

First Received: 21 June 2018;
Published Online: 4 March 2019

C. T. Sofocleous, MD, PhD, FSIR, FCIRSE
e-mail: sofoclec@mskcc.org

Treatment effectiveness generally is assessed with post-procedural anatomic contrast-enhanced imaging (ultrasound [US], computed tomography [CT], magnetic resonance imaging [MRI]) and/or metabolic imaging (positron emission tomography [PET]/CT).[9–11] However, LTP occurs even in the face of complete tumor ablation with sufficient margins by imaging (> 5 mm all around the target tumor).[5,10,12] This phenomenon can probably be attributed to the presence of residual viable tumor cells within the ablation zone that "escape" the spatial resolution of currently available morphologic and metabolic imaging.[12]

The presence of viable tumor cells in the ablation zone carries an increased risk for treatment failure and LTP, as well as shorter patient survival and cancer-specific survival.[12–17]Unlike surgical resection, ablative techniques are not routinely assessed or followed by pathologic assessment of the treated tumor and surrounding margins. Studies evaluating tissue adherent to radiofrequency electrodes after ablation have shown that the presence of viable/proliferating cells is an independent predictor of shorter LTP-free survival.[13,14,16,17] This was confirmed prospectively with biopsy of the ablation zone and pathologic assessment after tissue fixation using immunohistochemical (IHC) staining.[12]

All previous studies have shown a very strong correlation between the identification of viable or proliferating tumor cells and local tumor progression. However, routine tissue processing and pathologic examination requires days, and can take even longer with the use of IHC stains. Therefore, a common limitation of these described methods has been the inability to provide immediate tissue evaluation at the time of the ablation, precluding the possibility of additional ablation in the same session for treatment completion and tumor eradication.[18]

This prospective study aimed to evaluate whether rapid tissue examination (within 30 min after ablation and sampling) using fluorescent stains is feasible and correlates with known standard pathologic examinations showing viable tumor cells with already documented prognostic value in predicting LTP after hepatic tumor and specifically CLM ablation.[12–15]

MATERIALS AND METHODS

Patient Selection

This National Institutes of Health (NIH)-supported, institutional review board (IRB)-approved prospective study analyzed tissue collected from the center and margin of the ablation zone of CLM through core needle biopsies. Patients undergoing ablation of CLM were assessed for prospective enrollment in this Health Insurance Portability and Accountability Act-compliant study.

Patients eligible for enrollment were those who had up to three CLMs (each < 5 cm in largest diameter) and no more than three extrahepatic sites of disease. Patients with uncorrectable coagulopathy (international normalized ratio [INR] > 1.5 or a platelet count of < 50,000/mm^3) and those unable to undergo general anesthesia were not eligible for the study (Table 1).

Treatment

Between January 2011 and December 2014, 53 consecutive CLMs in 34 patients were treated with image-guided ablation. All procedures were performed with the patient under general anesthesia and with continuous monitoring by an anesthesiologist. The treatment methods used were radiofrequency (RF; n = 15), microwave (MW; n = 34), and irreversible electroporation (IRE; n = 4), depending on tumor size, shape, and location, as well as operator preference.

Electrode/applicator repositioning and overlapping ablations were performed to create an ablation zone with a minimum ablation margin of at least 5 mm uniformly around the target tumor. Electrode/applicator placement and accurate tumor targeting were performed under CT guidance aided by CT fluoroscopy and/or sonography whenever needed. In addition, PET/CT guidance was used in 41 of the 53 ablations.[19] In all cases, the manufacturer's recommended protocol was applied and completed.[20,21]

The RF devices used were the Valley-Lab Cool-Tip (n = 13; Covidien/Medtronic, Minneapolis, MN) and the RITA Starburst XLi (n = 2; Angiodynamics, Glens Falls, NY). The MW devices used were the NEUWAVE ablation system (n = 24; NeuWave Medical/Ethicon, Somerville, NJ), the Amica system (n = 5; Mermaid Medical, Centennial, CO), the Microsulis system (n = 4; Angiodynamics), and the Emprint system (n = 1; Covidien/Medtronic, Minneapolis, MN). The IRE device used was the Nanoknife System (n = 4; Angiodynamics, Glens Falls, NY). The mean number of ablation probes used per tumor was 1.7 (range, 1–4), and overlapping ablations were performed in 45 of the 53 cases (85%).

All the patients were assessed for complete tumor ablation immediately after the procedure and then 6 weeks (± 2 weeks) after the ablation with a triphasic contrast-enhanced CT. The ablation was considered technically successful when the ablation zone completely covered the target tumor.

Biopsy and Tissue Analysis

Immediately after completion of the tumor ablation, 18- to 20-gauge core biopsy specimens were collected from the center and the margin of the ablation zone using contrast-

TABLE 1 Concordance of sample classification as either tumor-negative or tumor-positive with immediate fluorescent stain evaluation and standard morphologic assessment using hematoxylin and eosin (H&E) by the study pathologist

Fluorescent stain evaluation	H&E evaluation		
	Tumor-positive	Tumor-negative	Total
Tumor-positive	18	4	22
Tumor-negative	0	41	41
Total	18	45	63

Discordance was observed in 4 cases, leading to an overall concordance rate of 94% (59/63). All 4 cases of discordant samples were false-positive at fluorescent stain evaluation

enhanced CT and/or PET/CT with fusion technology.[12] If available, tissue adherent to the electrodes also was collected.[15,16] For the purpose of this study, some of the tissue samples were submitted live (fresh) for immediate fluorescent analysis in the Molecular Cytology Core Facility and subsequently fixed for further morphologic and IHC analysis. Other biopsy tissue samples did not undergo fluorescent staining (only routine pathologic assessment) and are not discussed in this study.

A combination of fluorescent markers was used, including a nuclear fluorescent marker, Hoechst 33342 (blue fluorescent dye) and a mitochondria viability fluorescent marker, MitoTracker (MT) Red (red fluorescent dye), in an effort to detect live cancer cells in the ablation zone. These fluorescent dyes are often used for in vitro experiments but have also been applied to freshly excised tissues.[22] As a fluorescent reagent, MT Red labels functionally active mitochondria in live cells by detecting intact mitochondrial oxidative phosphorylation. Hoechst 33342 was added for counterstaining and labeling of all nuclei within the same tissue sample.

All collected tissue samples were incubated for 20 min in the staining solution consisting of DME media with 15 mmol of HEPES buffer, 10% fetal calf serum, 500 nmol of MitoTracker Red CM-H2XRos (Invitrogen, Thermo Fisher Scientific, Waltham, MA), and 10 μg/m of Hoechst 33342 (Sigma-Aldrich Corp., St Louis. MO). After incubation, the samples were mounted for imaging with an LSM 5 Live inverted confocal microscope (Zeiss, Oberkochen, Germany, San Diego, CA) using a × 20/0.8NA objective. A 579-nm laser line was used to excite MT Red and 405-nm laser line for Hoechst 33342. Several z-stacks per sample were obtained and reviewed.

Subsequently, exactly the same tissue samples were fixed in formalin, dehydrated, embedded in paraffin, cut into 5-μm sections, and stained with standard hematoxylin and eosin (H&E) morphologic stains.

The study pathologist searched for cancer cells in the sample by observing the morphologic characteristics of the Hoechst-stained nuclei combined with the presence of MT Red. Cancer cells were identified by the presence of densely distributed nuclei in Hoechst. When these were positive for MT Red, the classification of viable tumor was made (Fig. 1a). Hoechst staining of characteristically large round nuclei (normal hepatocytes) with matching strong MT Red staining resulted in their classification as normal liver tissue (Fig. 1b). Lack of MT Red signal in regions containing cells identified by the nuclear Hoechst stain resulted in their classification as nonviable/necrotic tissue. The fluorescent findings were validated by blinded comparison with the corresponding H&E morphologic stain, with additional IHC for identified tumor cells.

After H&E evaluation, the study pathologist, blinded to the interpretation of the fluorescent assessment, classified the same tissue samples as tumor cells, normal liver tissue, or coagulation necrosis. Specimens with morphologically identified tumor cells on standard H&E examination (n = 18) were further assessed with IHC stains for proliferation marker Ki67 and mitochondria viability marker OxPhos (OXP). This allowed further classification of identified cancer cells into viable tumor cells or coagulation necrosis, as well as direct correlations of MT Red and OXP positivity with cellular proliferation (Ki67-positive) and viability (OXP-positive). Incubation in primary antibodies against proliferation marker, Ki67 (0.4 μg/ml; Vector Labs Cat#VP-K451, Doral (Miami), FL) and OxPhos (2 μg/ml; Invitrogen Cat#459600), lasted 5 h.

After washing, chromogen-based detection was performed with the DAB MAP kit (Ventana Medical Systems, Tuscon, AZ) according to the manufacturer's instructions. The morphologic H&E classification combined with Ki67 and OXP immunohistochemistry was considered the gold standard reference for evaluation of the ablation zone and classification of the tissue into viable tumor cells, normal liver cells, and coagulation necrosis.

Statistical Analysis

The sensitivity, specificity, and overall concordance of fluorescent stain findings versus standard pathologic examination with H&E and IHC were calculated.

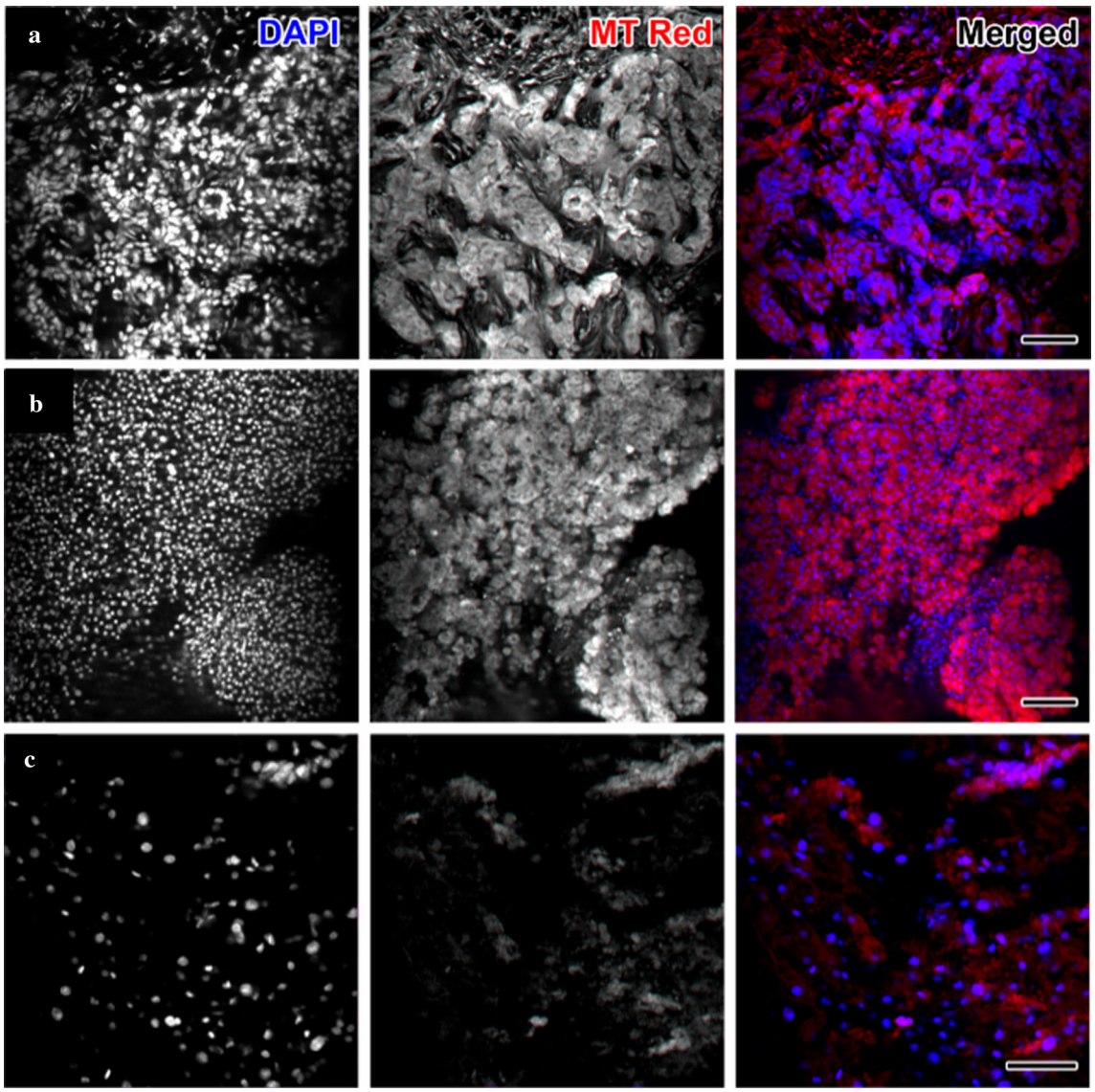

FIG. 1 Maximum projection of confocal stacks imaging tissues obtained from the ablation zone center. The left-most column presents the grayscale image of DAPI (nuclear) staining. The second column shows the grayscale image of MitoTracker Red staining. The third column shows the merged image. **a** The sample was classified by the study pathologist as highly suggestive of residual viable tumor cells within the ablation zone due to the evident MitoTracker Red positivity within the dense distribution of nuclei. The Ki67 and OxPhos immunohistochemical (IHC) staining corroborated this finding. **b** Hoechst staining showing characteristic large round nuclei of hepatocytes that are alive and normal due to strong MitoTracker Red staining. Samples such as this one were classified as normal tissue. **c** MitoTracker Red was considered negative in regions containing cells, as depicted by the nuclear Hoechst stain. Thus, this tissue sample was classified as nonviable. Hematoxylin and eosin (H&E) evaluation confirmed the presence of coagulative necrosis. Scale bar = 100 μm for all panels

RESULTS

A total of 63 tissue samples were collected and processed from 53 ablated CLMs in 34 patients. In all cases, imaging evidence showed technically successful, complete tumor ablation. Of the 63 specimens, 46 were obtained from the center of the ablation zone, 13 from the margin, and 4 from tissue adherent on the used ablation electrodes.

At immediate fluorescent assessment, 22 (35%) of the 63 specimens were considered positive for the presence of viable tumor cells. Morphologic H&E assessment showed that 18 (82%) of these 22 specimens contained tumor cells. The four false-positive samples identified as tumor cells on the fluorescent images corresponded to preserved cholangiocytes lining small bile ducts as shown on H&E. The distribution of the cholangiocytes around the bile duct was misinterpreted on the morphologic fluorescent images

(Hoechst) as indicating the glandular morphology of adenocarcinoma (Fig. 2). All 41 specimens (100%) classified as necrotic or non-cancerous at immediate fluorescent assessment displayed characteristics of complete coagulative necrosis or normal liver tissue on standard H&E morphologic assessment and did not undergo further processing with IHC.

The overall rate of concordance between immediate fluorescent stain interpretation and standard H&E examination for the detection of tumor versus coagulation necrosis and normal liver parenchyma was 94% (59/63). The fluorescent stain sensitivity for identifying samples positive for tumor on standard H&E was 100% (18/18), and specificity was 91% (41/45). Of the 18 specimens showing tumor cells on H&E that were further processed with IHC, 16 were positive for both markers Ki67 and OXP. One specimen was positive for only Ki67, and in one specimen, the collected tissue was inadequate for assessment with IHC.

DISCUSSION

The results of our study show that fluorescent MT Red and Hoechst stains used in rapid tissue analysis may be a potential immediate biomarker of complete ablation of liver tumor, particularly CLM. This combination addresses the disadvantage of each fluorescent stain when used separately. Although MT Red may distinguish viable from necrotic/apoptotic cells, it cannot differentiate benign from malignant cells. Nuclear labeling by Hoechst appears to provide a fluorescent equivalent of H&E and assists in the detection of neoplastic cells, but it cannot assess viability. The combination of the two stains provides the ability to interrogate rapidly for residual viable tumor cells, with a relatively high concordance rate (94%) compared with lengthy standard pathologic assessment.

We previously showed that Ki67-positive tumor cells adherent to the electrode after hepatic tumor RF ablation are associated with shorter LTP-free and overall survival. The presence of Ki67-positive tumor cells from the

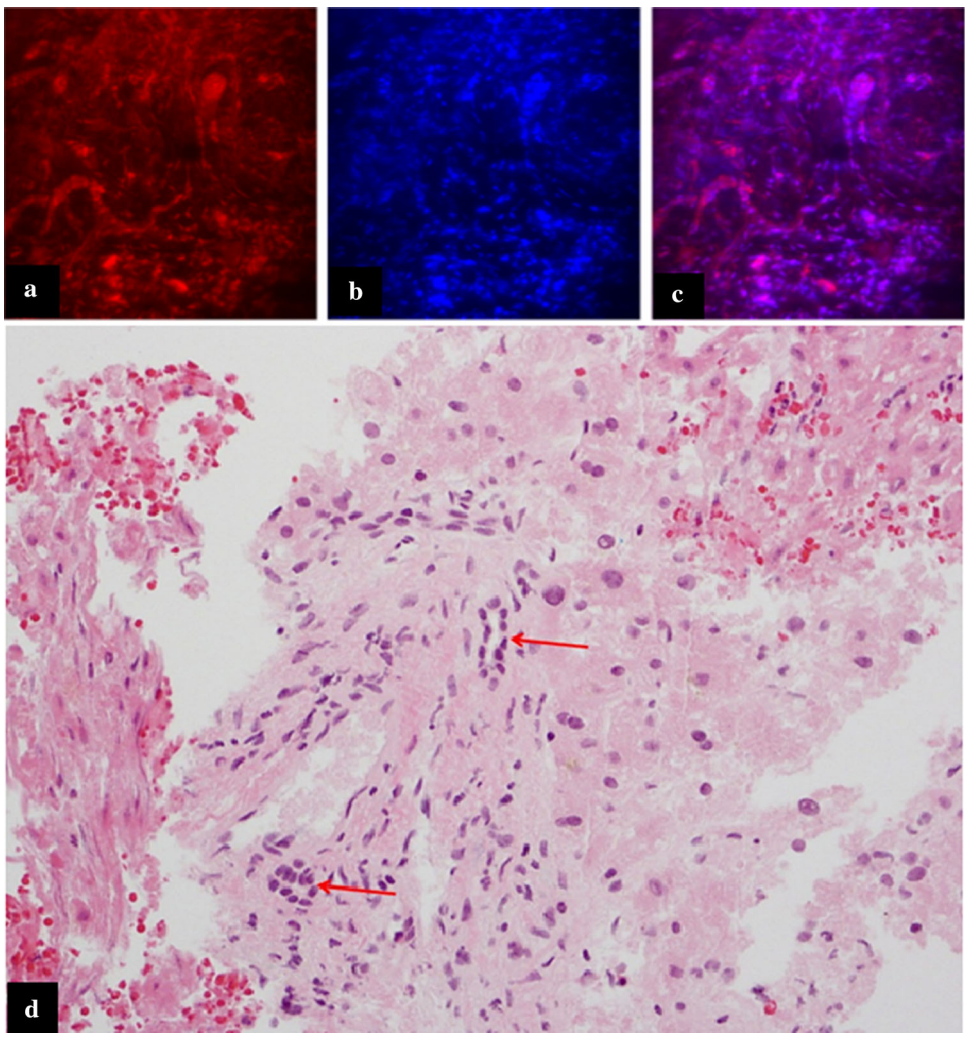

FIG. 2 False-positive case. Fluorescent images with **a** MitoTracker Red, **b** Hoechst, **c** composite image, and **d** corresponding hematoxylin and eosin (H&E). The fluorescent images were considered positive for tumor cells due to MitoTracker Red positivity in areas with dense distribution of nuclei. The standard pathologic examination H&E showed no evidence of adenocarcinoma. However, preserved cholangiocytes around bile ducts (red arrows) were observed, which likely were interpreted as tumor on the fluorescent images

ablation zone was an independent predictor of shorter LTP-free survival (hazard ratio, 5.1).[15] Snoeren et al.[16] analyzed the viability of tissue adherent to electrodes by the autofluorescence method using glucose-6-phosphate diaphorase staining and concluded that viable tissue is an independent risk factor for LTP. However, in all these studies, tissue evaluation was performed after fixation and lengthy processing.[13,15–17]

Tanis et al.[18] applied real-time reflectance spectroscopy during RF ablation in eight colon cancer live metastases, which indicated more than a 97% correlation with histopathologic changes of necrosis and subsequent CT imaging of complete tumor ablation. The authors highlighted the value of real-time feedback during tumor ablation that could significantly improve success rates and diminish LTP after ablation. The study did not assess for the presence of residual viable tumor at the end of ablation.

Fujisawa et al.[23] evaluated the use of YO-PRO-1, a green fluorescent DNA marker for cells with a compromised plasma membrane, as a potential immediate marker of cell death after RF ablation of CLM using biopsy samples from the ablation zone. More than 90% of the cells were positive for this marker after ablation. However, similar levels of YO-PRO-1 positivity were encountered in dissected non-ablated pig and mouse liver specimens, leading to the conclusion that YO-PRO-1 has limited value as a potential immediate biomarker of complete tumor ablation.

The fluorescent stains used in the current study assessed cell viability based on mitochondrial function. The combination of morphologic assessment with mitochondrial evaluation is extremely important and addresses several limitations pertaining to tissue assessment immediately after ablation. In particular, earlier work indicated that tumor cells identified within resected specimens after ablation could undergo further apoptosis and complete necrosis several days after RF ablation.[24] This made immediate assessment of ablated specimens extremely difficult and indicated the need for application of specific viability and apoptotic stains to assess the status of tumor cells accurately after ablation. Most of these stains require viable tumor processing with IHC that is lengthy and not easy to use as an immediate assay to detect residual viable tumor or necrosis. The development of such markers is critical because ablation is evolving as a cancer therapy with curative intent that could be offered instead of surgery.[5,11,25]

The ability to confirm complete tumor necrosis, and more importantly, the ability to detect residual viable tumor immediately after completion of ablation is essential for providing the best possible care. Identification of residual tumor cells immediately after therapy would allow for application of additional ablation while the patient remains under general anesthesia, provided a target is identified by imaging. When additional ablation is not safe or feasible, the immediate assessment would alert the treating physicians of the presence of residual tumor cells that dramatically increase the risk of treatment failure and tumor progression. In the latter scenario, adjuvant therapy could be initiated in a manner similar to the management of patients who undergo resection with tumor-positive margins.[26]

In our study, all procedures were performed until imaging evidence showed complete tumor ablation with adequate margins. The incidence of viable tumor cells in the post-ablation biopsy specimens did not differ significantly between ablation methods. In another study, we showed no difference in local tumor progression between RF and MW ablation when data were stratified by margin, although the ability to obtain margins was influenced in perivascular tumors treated with RF but not in those treated with MW.[27] Patients with viable tumor cells shown on the intraprocedural biopsy continued routine imaging follow-up evaluation and were retreated only if imaging evidence showed recurrence.

In this cohort, no treatment decision was made based on the results of the fluorescent stains. The implementation of fluorescent stains in the treatment paradigm will be part of a future clinical trial.

The limitations of our study included the relatively small number of specimens analyzed and the fact that pre-procedural biopsies were not obtained to allow comparison of fluorescent stains and imaging findings before and after ablation, or to allow correlation with known technical factors,[5,26,27] tumor markers, and genomic profiles[28–31] that may affect outcomes. The evaluation performed with biopsies remains incomplete and may miss areas of residual viable tumor within the ablation zone or the margins, especially if compared with completely excised specimens.[12] Moreover, this was a proof-of-concept study investigating the use of fluorescent stains for rapid tissue assessment. This precliminary study was not designed to determine whether the presence of cells considered malignant and viable with these stains places patients at increased risk for local recurrence. Finally, the fluorescent images and pathology slides were interpreted by a single pathologist, precluding assessment of interobserver variability.

In summary, given the documented prognostic value of tissue characteristics for local tumor progression-free and overall survival for patients with CLM, ablation zone tissue evaluation with fluorescent stains appears to provide an intra-procedural biomarker of residual tumor or complete image-guided tumor ablation. This development could address a key limitation of ablation and potentially other image-guided locoregional therapies.

ACKNOWLEDGMENT This study was supported by the National Cancer Institute (Grant R21 CA131763-01A1). We gratefully acknowledge Alessandra Garcia, BA (Research Study Assistant at Memorial Sloan Kettering Cancer Center) for her contribution to this work.

DISCLOSURE This study was funded in part by NIH/NCI R21 CA131763-01A1 grant and it was presented at the RSNA annual meeting in Chicago November 28th–December 3rd, 2014. Memorial Sloan Kettering Cancer Center is supported by the grant P30 CA008748 from the National Cancer Institute (NCI). Authors Vlasios S. Sotirchos, Sho Fujisawa, Efsevia Vakiani and Katia O. Manova-Todorova indicated no conflict of interest (COI) disclosures to report. Dr. Stephen B. Solomon has reported the following industry relations and potential COI: Consulting: BTG, Johnson & Johnson, Adgero, Aperture Medical, XACT Robotics, Innoblative. Research Support: GE Healthcare, AngioDynamics, Johnson & Johnson, Elesta. Shareholder: Aspire Bariatrics, Aperture Medical, Johnson & Johnson, Immunomedics. Dr. Constantinos T. Sofocleous has reported the following industry relations and potential COI: Consulting: Neuwave/Ethicon Johnson & Johnson, Terumo Medical, GE Healthcare. Research Support: Neuwave/Ethicon Johnson & Johnson; Angiodynamics, HS Medical, BTG.

REFERENCES

1. Herszenyi L, Tulassay Z. Epidemiology of gastrointestinal and liver tumors. *Eur Rev Med Pharmacol Sci*. 2010;14:249–258. http://www.ncbi.nlm.nih.gov/pubmed/20496531.
2. Arnaud JP, Dumont P, Adloff M, Leguillou A, Py JM. Natural history of colorectal carcinoma with untreated liver metastases. *Surg Gastroenterol*. 1984;3:37–42. http://www.ncbi.nlm.nih.gov/pubmed/6522907.
3. Adam R, Vinet E. Regional treatment of metastasis: surgery of colorectal liver metastases. *Ann Oncol*. 2004;15(Suppl 4):iv103–6. https://doi.org/10.1093/annonc/mdh912.
4. Alberts SR, Poston GJ. Treatment advances in liver-limited metastatic colorectal cancer. *Clin Colorectal Cancer*. 2011;10:258–65. https://doi.org/10.1016/j.clcc.2011.06.008.
5. Shady W, Petre EN, Gonen M, et al. Percutaneous radiofrequency ablation of colorectal cancer liver metastases: factors affecting outcomes: a 10-year experience at a single center. *Radiology*. 2016;278:601–11. https://doi.org/10.1148/radiol.2015142489.
6. Solbiati L, Livraghi T, Goldberg SN, et al. Percutaneous radiofrequency ablation of hepatic metastases from colorectal cancer: long-term results in 117 patients. *Radiology*. 2001;221:159–66. https://doi.org/10.1148/radiol.2211001624.
7. Hanna NN. Radiofrequency ablation of primary and metastatic hepatic malignancies. *Clin Colorectal Cancer*. 2004;4:92–100. https://doi.org/10.3816/ccc.2004.n.012.
8. White RR, Avital I, Sofocleous CT, et al. Rates and patterns of recurrence for percutaneous radiofrequency ablation and open wedge resection for solitary colorectal liver metastasis. *J Gastrointest Surg*. 2007;11:256–63. https://doi.org/10.1007/s11605-007-0100-8.
9. Cornelis F, Sotirchos V, Violari E, et al. 18F-FDG PET/CT is an immediate imaging biomarker of treatment success after liver metastasis ablation. *J Nucl Med*. 2016;57:1052–7. https://doi.org/10.2967/jnumed.115.171926.
10. Wang X, Sofocleous CT, Erinjeri JP, et al. Margin size is an independent predictor of local tumor progression after ablation of colon cancer liver metastases. *Cardiovasc Intervent Radiol*. 2013;36:166–75. https://doi.org/10.1007/s00270-012-0377-1.
11. Solbiati L, Ahmed M, Cova L, Ierace T, Brioschi M, Goldberg SN. Small liver colorectal metastases treated with percutaneous radiofrequency ablation: local response rate and long-term survival with up to 10-year follow-up. *Radiology*. 2012;265:958–68. https://doi.org/10.1148/radiol.12111851.
12. Sotirchos VS, Petrovic LM, Gönen M, et al. Colorectal cancer liver metastases: biopsy of the ablation zone and margins can be used to predict oncologic outcome. *Radiology*. 2016;280:949–59. https://doi.org/10.1148/radiol.2016151005.
13. Sofocleous CT, Garg S, Petrovic LM, et al. Ki-67 is a prognostic biomarker of survival after radiofrequency ablation of liver malignancies. *Ann Surg Oncol*. 2012;19:4262–9. https://doi.org/10.1245/s10434-012-2461-9.
14. Sofocleous CT, Garg SK, Cohen P, et al. Ki 67 is an independent predictive biomarker of cancer specific and local recurrence-free survival after lung tumor ablation. *Ann Surg Oncol*. 2013;20(3 Suppl):S676–83. https://doi.org/10.1245/s10434-013-3140-1.
15. Sofocleous CT, Nascimento RG, Petrovic LM, et al. Histopathologic and immunohistochemical features of tissue adherent to multitined electrodes after RF ablation of liver malignancies can help predict local tumor progression: initial results. *Radiology*. 2008;249:364–74. https://doi.org/10.1148/radiol.2491071752.
16. Snoeren N, Huiskens J, Rijken AM, et al. Viable tumor tissue adherent to needle applicators after local ablation: a risk factor for local tumor progression. *Ann Surg Oncol*. 2011;18:3702–10. https://doi.org/10.1245/s10434-011-1762-8.
17. Snoeren N, Jansen MC, Rijken AM, et al. Assessment of viable tumour tissue attached to needle applicators after local ablation of liver tumours. *Dig Surg*. 2009;26:56–62. https://doi.org/10.1159/000194946.
18. Tanis E, Spliethoff JW, Evers DJ, et al. Real-time in vivo assessment of radiofrequency ablation of human colorectal liver metastases using diffuse reflectance spectroscopy. *Eur J Surg Oncol*. 2015;42:251–9. https://doi.org/10.1016/j.ejso.2015.12.005.
19. Ryan ER, Sofocleous CT, Schöder H, et al. Split-dose technique for FDG PET/CT-guided percutaneous ablation: a method to facilitate lesion targeting and to provide immediate assessment of treatment effectiveness. *Radiology*. 2013;268:288–95. https://doi.org/10.1148/radiol.13121462.
20. Sofocleous CT, Sideras P, Petre EN. How we do it: a practical approach to hepatic metastases ablation techniques. *Tech Vasc Interv Radiol*. 2013;16:219–29. https://doi.org/10.1053/j.tvir.2013.08.005.
21. Ahmed M, Solbiati L, Brace CL, et al. Image-guided tumor ablation: standardization of terminology and reporting criteria: a 10-year update. *Radiology*. 2014;273:241–60. https://doi.org/10.1148/radiol.14132958.
22. Boffa DJ, Waka J, Thomas D, et al. Measurement of apoptosis of intact human islets by confocal optical sectioning and stereologic analysis of YO-PRO-1-stained islets. *Transplantation*. 2005;79:842–5. https://doi.org/10.1097/01.tp.0000155175.24802.73.
23. Fujisawa S, Romin Y, Barlas A, et al. Evaluation of YO-PRO-1 as an early marker of apoptosis following radiofrequency ablation of colon cancer liver metastases. *Cytotechnology*. 2014;66:259–73. https://doi.org/10.1007/s10616-013-9565-3.
24. Goldberg SN, Gazelle GS, Compton CC, Mueller PR, Tanabe KK. Treatment of intrahepatic malignancy with radiofrequency ablation: radiologic-pathologic correlation. *Cancer*. 2000;88:2452–63. https://doi.org/10.1002/1097-0142(20000601)88:11%3c2452::aid-cncr5%3e3.0.co;2-3.
25. Tanis E, Nordlinger B, Mauer M, et al. Local recurrence rates after radiofrequency ablation or resection of colorectal liver metastases: analysis of the European Organisation for Research

and Treatment of Cancer #40004 and #40983. *Eur J Cancer*. 2014;50:912–9. https://doi.org/10.1016/j.ejca.2013.12.008.
26. Mbah NA, Scoggins C, McMasters K, Martin R. Impact of hepatectomy margin on survival following resection of colorectal metastasis: the role of adjuvant therapy and its effects. *Eur J Surg Oncol*. 2013;39:1394–9. https://doi.org/10.1016/j.ejso.2013.09.009.
27. Shady W, Petre EN, Do KG, et al. Percutaneous microwave versus radiofrequency ablation of colorectal liver metastases: ablation with clear margins (A0) provides the best local tumor control. *J Vasc Interv Radiol*. 2018;29(2):268–275. https://doi.org/10.1016/j.jvir.2017.08.021.
28. Shady W, Petre EN, Vakiani E, et al. Kras mutation is a marker of worse oncologic outcomes after percutaneous radiofrequency ablation of colorectal liver metastases. *Oncotarget*. 2017;8:66117–27. https://doi.org/10.18632/oncotarget.19806.
29. Ziv E, Bergen M, Yarmohammadi H, et al. PI3K pathway mutations are associated with longer time to local progression after radioembolization of colorectal liver metastases. *Oncotarget*. 2017. https://doi.org/10.18632/oncotarget.15278.
30. Calandri M, Yamashita S, Gazzera C, et al. Ablation of colorectal liver metastasis: interaction of ablation margins and RAS mutation profiling on local tumour progression-free survival. *Eur Radiol*. 2018. https://doi.org/10.1007/s00330-017-5273-2.
31. Odisio BC, Yamashita S, Huang SY, et al. Local tumour progression after percutaneous ablation of colorectal liver metastases according to RAS mutation status. *Br J Surg*. 2017;104:760–8. https://doi.org/10.1002/bjs.10490.